Available online at www.sciencedirect.com
ScienceDirect
Theoretical Population Biology 70 (2006) 527–541
Theoretical Population Biology
www.elsevier.com/locate/tpb

Advantage of storage in a fluctuating environment

B.W. Kooi*, T.A. Troost[1]

Department of Theoretical Biology, Vrije Universiteit, de Boelelaan 1087, 1081 HV Amsterdam, The Netherlands

Received 15 January 2006
Available online 10 August 2006

Abstract

We will elaborate the evolutionary course of an ecosystem consisting of a population in a chemostat environment with periodically fluctuating nutrient supply. The organisms that make up the population consist of structural biomass and energy storage compartments. In a constant chemostat environment a species without energy storage always out-competes a species with energy reserves. This hinders evolution of species with storage from those without storage. Using the adaptive dynamics approach for non-equilibrium ecological systems we will show that in a fluctuating environment there are multiple stable evolutionary singular strategies (ss's): one for a species without, and one for a species with energy storage. The evolutionary end-point depends on the initial evolutionary state. We will formulate the invasion fitness in terms of Floquet multipliers for the oscillating non-autonomous system. Bifurcation theory is used to study points where due to evolutionary development by mutational steps, the long-term dynamics of the ecological system changes qualitatively. To that end, at the ecological time scale, the trait value at which invasion of a mutant into a resident population becomes possible can be calculated using numerical bifurcation analysis where the trait is used as the free parameter, because it is just a bifurcation point. In a constant environment there is a unique stable equilibrium for one species following the "competitive exclusion" principle. In contrast, due to the oscillatory dynamics on the ecological time scale two species may coexist. That is, non-equilibrium dynamics enhances biodiversity. However, we will show that this coexistence is not stable on the evolutionary time scale and always one single species survives.

Keywords: Adaptive dynamics; Bifurcation analysis; Coevolution; Ecosystem dynamics; Energy storage; Periodically fluctuating environment

1. Introduction

Many species store energy extracted from food via assimilation before they use it for growth and maintenance. Droop (1973) introduced the concept of cell nutrient quota (internal nutrient density) besides biomass in a model for phytoplankton growth. In this model growth is decoupled from nutrient uptake. It assumes that phytoplankton cells store nutrient and that the growth rate depends on the amount of stored nutrient. More recently models were proposed where also two components in an organism are distinguished. In Hallam et al. (1990) a model is described where an organism consists of storage (lipids, the major source of energy) and a structural component (non-lipid dry material consisting mostly of proteins and carbohydrates). The Dynamic Energy Budget (DEB) model Kooijman (2000), deals with storage materials (reserves) and structural biomass. Here the storage materials are carbohydrates and lipids but also a part of ribosomal RNA and of the proteins Kooijman (2000). The storage materials have a dual function as a reserve pool for energy and elementary compounds. All assimilates enter the reserve compartment. The reserve energy is used for maintenance, growth and reproduction. In Noonburg et al. (1998) this model is called the *net assimilation* model and is compared to another DEB model called *net production* model where maintenance is payed from assimilates first and the rest enters the reserve pool from which it is used for growth and reproduction.

The main issue discussed in this paper is the evolution of energy storage. In Shertzer and Ellner (2002) this issue is discussed for an ecosystem consisting of algae and rotifers. The chemostat is kept in the dark and therefore the

*Corresponding author. Fax: +31 20 5987123.
E-mail addresses: kooi@bio.vu.nl (B.W. Kooi), tineke@bio.vu.nl (T.A. Troost).
[1]Present address: Royal Netherlands Institute of Sea Research, Department of Marine Ecology and Evolution, P.O. Box 59, Den Burg, Texel NL-1790 AB, Netherlands.

0040-5809/$ - see front matter © 2006 Elsevier Inc. All rights reserved.
doi:10.1016/j.tpb.2006.07.005

supplied algae are non-vital. To model the dynamics of the rotifer population with two life stages, juveniles and adults, a physiological structured population (partial differential equation PDE) model based on a net production DEB model was formulated. The model studied here is a simplified version of the model described in Kooi and Kooijman (1999) for a algae-rotifers system in the chemostat. The two life stage of the rotifers are now embryonic and adult. The adults do not grow but use all energy extracted from assimilates for reproduction. Furthermore the egg development time is assumed to be short. As a result the final mathematical model becomes unstructured (set of coupled ordinary differential equations (ODE's)).

We use the adaptive dynamics approach (Metz et al., 1996; Geritz et al., 1998, 1999) to determine the evolutionary process by small mutational steps. The adaptive trait under consideration is the maximum energy storage size. We derive the invasion fitness using a stability analysis of the resident population where the mutant population, albeit with zero structural biomass, is taken into account, as well as feedback via the nutrients. For periodically fluctuating environments the invasion fitness is positive when the magnitude of the dominant Floquet multiplier of the system's monodromy matrix evaluated at the periodic solution is greater than 1 and negative when it is less than 1. We define the invasion rate $s = \log(\mu_1)$ where μ_1 is the magnitude of the dominant Floquet multiplier evaluated at the periodic solution of the resident system where the size of the mutant population is zero (Metz et al., 1992). In biological terms, it is the average of the invasion rate during one cycle period. The Floquet multipliers are calculated with bifurcation analysis packages such as Locbif Khibnik et al. (1993) (the module called "Periodic solutions of non-autonomous time-periodic ODEs") or AUTO (Doedel et al., 1997).

Invasion of the mutant leads to replacement of the resident population or establishment besides the resident population. In the latter case further analysis is needed of the invasibility at the resulting dimorphic population.

The derived invasion gradients are substituted into the canonical equations (Dieckmann and Law, 1996) that describe the dynamics of the trait. This allows for calculation of the evolutionary end-point.

In a constant environment a species that uses assimilates directly for maintenance and growth out-competes a species that stores these assimilates into a reserve pool before using it for maintenance, growth and reproduction. However, in a fluctuating environment, having an energy storage can be beneficial in order to survive periods of food deprivation.

With a highly periodically fluctuating algae supply, the analysis reveals bi-stability of two monomorphic stable (both convergence and evolutionary) ss's; one with and the other without an energy storage compartment. These two ss's are separated by an (both convergence and evolutionary) unstable ss. So, on the evolutionary time scale always one single species survives: it depends on the initial conditions at which evolution ends in a convergence and evolutionary stable ss. The unstable point hinders the evolutionary step from a simpler species without storage into a more complex species with storage.

The paper is organized as follows. In Section 2 the model is formulated starting at the individual level and thereafter at the population level. The model for organisms with and without storage are derived as set of coupled ODEs. At the ecological time scale the size of the energy storage is constant. In Section 3 it is subject to small mutational changes at the evolutionary time scale. The invasion fitness of a mutant population invading a resident population is derived in Section 4 for a constant environment and thereafter for a periodically fluctuating environment. The evolutionary course is analysed in Section 5. In Section 6 the effects of the amplitude of the fluctuations of the environment are studied.

2. Ecological time-scale equations

In the DEB model (Kooijman, 2000) the organism is partitioned (and consequently also the population) into two compartments: structure and energy reserves. We assume that three chemical transformation processes take place in the individual; assimilation $\mathscr{A}$, maintenance $\mathscr{D}$ and growth and/or reproduction $\mathscr{G}$ (Kooi and Hanegraaf, 2001)

$$X_X \xrightarrow{\mathscr{A},v} X_E + X_A, \quad X_E \xrightarrow{\mathscr{D},m} X_D, \quad X_E \xrightarrow{\mathscr{G},g} X_V + X_G. \tag{1}$$

Reserve material, X_E, is generated from the nutrient, X_X, by the assimilation process. The energy stored in the reserve materials is used in the maintenance process and the growth and/or reproduction process whereby structural material, X_V, is formed. Non-limiting nutrients are consumed in these chemical processes and products are formed. In the mathematical description they differ only in sign. So, for each process, $\mathscr{P} \in \{\mathscr{A}, \mathscr{D}, \mathscr{G}\}$, we can combine these materials and call them "products". These combined products are denoted by X_A, X_D and X_G for the assimilation (faeces), maintenance (e.g. oxygen consumption and carbon dioxide production) and growth and/or reproduction process, respectively.

There are two rate parameters v (the energy conductance), m (maintenance rate coefficient) and the parameter g (the energy investment ratio), one for each of the three processes, indicated in (1). When I is the maximum ingestion rate by which the nutrient is consumed by the organism, then the rate v describes the conversion of nutrient into reserve material (Kooi and Hanegraaf, 2001, Eq. (12)),

$$v = \frac{I}{\eta_{X,\mathscr{A}} \tilde{\mu}_E [M_{Em}]}, \tag{2}$$

where $\eta_{X,\mathscr{A}}$ is the stoichiometric constant for the nutrient mass flux into energy reserve flux and $\tilde{\mu}_E$ is the chemical potential of the reserves and $[M_{Em}]$ is the maximum reserves mass per structural mass which is assumed to be

species specific. The brackets indicate that it is expressed per structural mass. The energetic costs for maintenance are proportional to the structural component while reserves do not need to be maintained.

The parameter g describes the conversion of reserve energy into structural biomass (Kooi and Hanegraaf, 2001, Eq. (12)),

$$g = \frac{1}{\eta_{V\mathscr{G}} \tilde{\mu}_E [M_{Em}]}, \tag{3}$$

where $\eta_{V\mathscr{G}}$ is the stoichiometric constant for the energy reserve flux in to structural biomass flux. It is associated with how much energy the synthesis of biomass costs. These parameters are defined at the individual level but can straightforwardly be used at the population level as follows.

We consider algae consumed by a rotifer population in the chemostat. The algae live in the dark, and therefore, they are non-vital. The rotifers have two stages, an egg and an adult stage. The adults do no grow and allocate all energy extracted from the algae to reproduction. So, the population growth rate is solely due to an increase in biomass and energy reserves via newborns. Adults are removed from the chemostat reactor with the dilution rate D. With continuous reproduction the dynamics of the rotifer population is described by a delay differential equation (DDE) system where the egg development time is the delay. In this paper we simplify this even further assuming a negligible time delay: in other words, we assume that the egg development is very fast and all energy available for reproduction is immediately used for reproduction. Consequently, all energy available for reproduction is immediately also used for reproduction (see Kooi and Kooijman, 1999). Then we obtain for the non-vital algae population and the rotifer population the ODE system (4).

Let $x_0 \geqslant 0$ be the concentration of algae. Let $x_1 \geqslant 0$ be the population structural (adult) biomass and $0 \leqslant e_1 \leqslant 1$ the scaled (with respect to a species specific maximum energy density) energy reserves of the population in a chemostat. The population model at the ecological time-scale reads

$$\frac{dx_0}{dt} = (x_r(t) - x_0)D - If(x_0)x_1, \tag{4a}$$

$$\frac{de_1}{dt} = v(f(x_0) - e_1), \tag{4b}$$

$$\frac{dx_1}{dt} = (\mathscr{M}(e_1) - D)x_1. \tag{4c}$$

The time dependent concentration of algae in the inflow is given by $x_r(t) = x_{r0}(\max(1 + \varepsilon \sin(2\pi t/T_0), 0))$ and T_0 the period of the excitation. The parameter D is the dilution rate. The Holling type II functional response,

$$f(x_0) = \frac{x_0}{k + x_0} \tag{5}$$

describes the trophic interaction between the rotifers and the algae. The per capita rotifer (population) growth rate reads

$$\mathscr{M}(e_1) = \frac{ve_1 - mg}{g_+ + e_1}, \quad g_+ = g + \frac{3mg}{4v}, \tag{6}$$

where g is the energy investment ratio and g_+ the cost of reproducing an egg. The second term in the expression for g_+ models additional costs associated with the maintenance during egg development which still have to be payed by the mother besides an amount of energy equal to her own reserves. We implicitly assume that all rotifer individuals have the same reserve energy density e_1. This can be justified as follows. Let two rotifer individuals have a different energy density. Then it is easy to see that the ODE (4b), which is linear in e_1, implies that this difference becomes exponentially smaller with time, whereby the decay rate is fixed by the specific-energy conductance v. When v is large with respect to the population growth rate, μ, the differences for all individuals are negligible small already during the individuals life time.

When $\mathscr{M}(e_1) < 0$ energy already allocated to reproduction is used to pay maintenance costs (and we implicitly assume that this energy can be retrieved with 100% effective, Kooi and Hanegraaf, 2001).

Model (4) becomes the unstructured DEB model (Kooijman, 2000) used for a population which propagates by binary fission when, in addition to no time delay, $g_+ = g$ holds. That is, the mother does not need to pay for the maintenance during the egg development since there are only adults in case of binary fission.

The ratio $\mu = v/g = I\eta_{V\mathscr{G}}/\eta_{X\mathscr{A}}$ is called the maximum population growth rate. Generally $y = \mu/I = \eta_{V\mathscr{G}}/\eta_{X\mathscr{A}}$ is called the efficiency (Ecology) or yield (Microbiology) which is constant by definition.

In what follows we are also interested in a special case where $\tilde{\mu}_E[M_{Em}] \to 0$, in which limiting case the size of the storage is zero. Then $v \to \infty$ and $g \to \infty$ while the ratio $v/g = \mu$ is finite. This means that the conversion from nutrients into reserves, fixed by rate v, is a fast process with respect to the growth and/or reproduction process which are fixed by rate μ. In quasi-steady-state, where $f(x_0) = e_1$, (4b) becomes an algebraic equation and we obtain the two-dimensional system

$$\frac{dx_0}{dt} = (x_r(t) - x_0)D - If(x_0)x_1, \tag{7a}$$

$$\frac{dx_1}{dt} = (\mu f(x_0) - m - D)x_1. \tag{7b}$$

Observe that the maximum growth rate is attained when food is abundant $f = e_1 = 1$ and no maintenance costs are paid, $m = 0$, while $g \gg 1$. This limiting case describes the dynamics of a population without energy storage and without maintenance costs.

This finalises the model formulation. In what follows we will use nutrient instead of algae and population instead of rotifers to stress that this model can be used for other organisms as well.

2.1. Dynamics of the ecosystem model

First, we consider a constant environment, $\varepsilon = 0$, where the equilibrium is a point attractor. For system (4) we obtain the stable equilibrium

$$\bar{x}_0 = \frac{f(\bar{x}_0)k}{1 - f(\bar{x}_0)}, \tag{8a}$$

$$\bar{x}_1 = \frac{(x_r - \bar{x}_0)D}{If(\bar{x}_0)}, \tag{8b}$$

$$\bar{e}_1 = f(\bar{x}_0) = \frac{mg + D\left(g + \dfrac{3mg}{4v}\right)}{v - D}. \tag{8c}$$

In the limiting case where $\tilde{\mu}_E[M_{Em}] \to 0$ we have in equilibrium

$$f(\bar{x}_0) = \frac{m + D}{\mu}, \tag{9}$$

together with (8a) and (8b).

When the nutrient concentration x_r in the inflow fluctuates, the system is non-autonomous. By a numerical analysis we found for all points in the environmental parameter space, (x_r, D), for system (4) with positive solutions that the periodic solution with period equal to the excitation period T_0 is stable. A transcritical bifurcation for the periodic solution forms the boundary for the region in the parameter space where the periodic solution is strictly positive.

Fig. 1 shows the two-parameter bifurcation diagram with x_r and D as bifurcation parameters. It shows two transcritical bifurcations TC for the reference values of the parameters given in Table 1, one for a constant ($\varepsilon = 0$) and one for a fluctuating ($\varepsilon = 1$) environment. Both curves are almost the same.

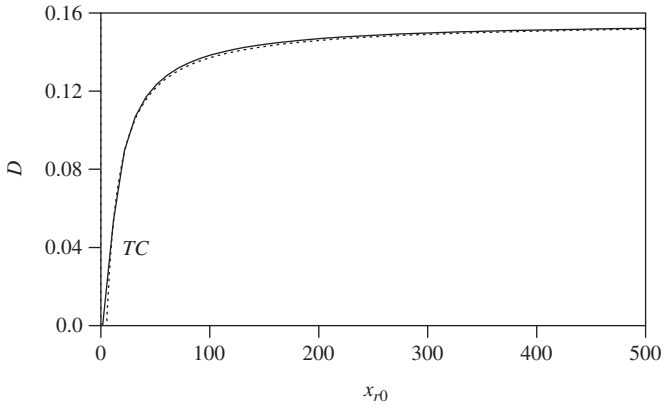

Fig. 1. Two-parameter bifurcation diagram for the chemostat system with x_{r0} and D as bifurcation parameters. All parameter values are given in Table 1. The solid line is the transcritical bifurcation curve TC for the equilibrium with $\varepsilon = 0$, that is constant nutrient supply. The dashed line is the transcritical bifurcation curve TC for the periodic solution with $\varepsilon = 1$. Except for a region close to the origin both transcritical bifurcation curves are similar.

3. Evolutionary time-scale equations

In the ecological model all parameters are constant. To study the evolutionary aspects of having a storage, we take the size of the storage as an adaptive trait. As the size of the storage we use the maximum reserves mass per structural mass, that is, the trait denoted by l, is defined by

$$l = \tilde{\mu}_E[M_{Em}]. \tag{10}$$

To study the system's evolutionary dynamics, we study whether a mutant with trait l_m may invade the resident population that has trait l_r. For this purpose we add two equations to the system, corresponding to the mutant biomass x_{1m} and mutant reserves e_{1m}.

$$\frac{dx_0}{dt} = (x_r(t) - x_0)D - If(x_0)x_{1r} - If(x_0)x_{1m}, \tag{11a}$$

$$\frac{de_{1r}}{dt} = \frac{\mu}{\eta_{V\mathscr{G}} l_r}(f(x_0) - e_{1r}), \tag{11b}$$

$$\frac{dx_{1r}}{dt} = \left(\frac{\mu e_{1r} - m}{1 + \left(\dfrac{3m}{4\mu} + e_{1r}\right)\eta_{V\mathscr{G}} l_r} - D\right)x_{1r}, \tag{11c}$$

$$\frac{de_{1m}}{dt} = \frac{\mu}{\eta_{V\mathscr{G}} l_m}(f(x_0) - e_{1m}), \tag{11d}$$

$$\frac{dx_{1m}}{dt} = \left(\frac{\mu e_{1m} - m}{1 + \left(\dfrac{3m}{4\mu} + e_{1m}\right)\eta_{V\mathscr{G}} l_m} - D\right)x_{1m}. \tag{11e}$$

The mutant population possesses the same parameter values as the resident except for the trait l.

A time scale separation is assumed, such that a new mutant occurs after the system is in the ecological stationary solution of system (11). This solution is an equilibrium for the autonomous system with $\varepsilon = 0$ and a periodic solution with period T_0 for the non-autonomous system.

In the case of non-equilibrium ecosystems an additional assumption has to be made (Dieckmann and Law, 1996). The extra requirement is that the mutant invasion is slow with respect to the period. As a result mutant extinction or fixation occurs only after many cycles.

The dynamics of the trait l_r are described by the canonical equation (Dieckmann and Law, 1996; Doebeli and Dieckmann, 2000; Dercole, 2003; Dercole et al., 2003)

$$\frac{dl_r}{d\tau} = \kappa \bar{x}_{1r} \left.\frac{\partial s(l_r, l_m)}{\partial l_m}\right|_{l_m = l_r}, \tag{12}$$

where τ is the time at the evolutionary time scale. The function s that depends on the trait value of the resident

Table 1
List of symbols and parameter values

Symbol	Dimension	Interpretation	Value
D	t^{-1}	Dilution rate	0.00135
e_1	—	Storage energy density	
f	—	Scaled functional response: $f = x_0/(k + x_0)$	
g	—	Energy investment ratio; $g_+ = g + \frac{3}{4}mg/v$	$0.025/l$
I	$mm^{-1}t^{-1}$	Maximum ingestion rate	1.3
k	mV^{-1}	Saturation coefficient	100
v	t^{-1}	Specific-energy conductance	$0.125/l$
m	t^{-1}	Maintenance rate coefficient	0.25
l	$e\,m^{-1}$	Trait value	0.71
t,τ	t	Time: ecological, evolutionary time-scale	
T_0	t	Excitation period	24
x_0	mV^{-1}	Algal density	
x_{r0}	L^3V^{-1}	Mean algal density in the input	500
x_1	mV^{-1}	Structural volume density of rotifers	
$[M_{Em}]$	mm^{-1}	Maximum mass reserves per structural mass	
η_{XA}	me^{-1}	Flux nutrient mass per flux assimilation energy	10.4
η_{VG}	me^{-1}	Flux biomass per flux energy for growth	40
μ	t^{-1}	Maximum population growth rate	
$\tilde{\mu}_E$	em^{-1}	Chemical potential of reserves	

The symbols in the column labeled 'dimension' stand for: t, time, e, energy, V, volume of reactor, m, biomass. Units are: mass densities in $\mu g\,ml^{-1}$ and rates in h^{-1}.

and mutant population is the invasion fitness. It will be derived in the next section for a constant and periodic environment as a growth rate of the mutant population. The parameter κ is the invasion rate coefficient and is proportional to the frequency of the mutations and the size of the mutational steps.

In the case of a monomorphic population there is one resident and in the dimorphic case there are two residents. In the dimorphic case a new mutant with trait values l_m tries to invade two resident populations with trait values $l_{ri}, i = 1, 2$. Then the evolutionary dynamics are described by the canonical equations

$$\frac{dl_{ri}}{d\tau} = \kappa_i \bar{x}_{1ri} \frac{\partial s_i(l_{r1}, l_{r2}, l_m)}{\partial l_m}\bigg|_{l_m = l_{ri}}, \tag{13}$$

where the parameter κ_i is the invasion rate coefficient of the mutant via the progenitor resident with trait l_{ri}. We assume that the two mutation distributions (Dieckmann and Law, 1996) are independent. In both expressions (12) and (13) the equilibrium structural biomass of the resident population has to be replaced by the cycle average for non-autonomous systems.

4. Derivation of the invasion fitness

Criteria for invasion of a mutant are derived: first via a point attractor in the autonomous case and then for a periodic solution attractor in the non-autonomous case.

4.1. Constant environment

We consider a system consisting of the nutrient, the resident population and the mutant population. The dimension of the system consisting of one ODE for the nutrient and two ODEs for each population, equals five. In order to investigate invasion of a mutant, the stability of the attractor on the boundary of the positive cone, where the nutrient density and the biomass and energy density of the resident population are positive, has to be considered as part of the system where the biomass of the mutant is zero. These attractors are stable with respect to the virgin three-dimensional system where no mutant is taken into account, only the nutrient and the resident population. The technique to derive the invasion fitness of the mutant population is based on the procedure worked out in Smith and Waltman (1994) and Kooi et al. (1999) for invasion of a top-predator into a food chain.

The stable equilibrium of ecosystem (11) with the mutant population taken into account, is denoted by

$$E_0 = (\bar{x}_0 \;\; \bar{e}_{1r} \;\; \bar{x}_{1r} \;\; \bar{e}_{1m} \;\; \bar{x}_{1m})^T, \tag{14}$$

where $\bar{x}_{1m} = 0$ and $\bar{e}_{1m} = \bar{e}_{1r} = f(\bar{x}_0)$ given by Eq. (8c). At the point of invasion, the mutant is identical to its progenitor resident except for the trait l. The Jacobian matrix evaluated at this equilibrium point has zero's such that the determinant possesses two linear factors associated with the dynamics of the mutant population. From this we can conclude directly that there are two eigenvalues in addition to the three of the original system without mutant,

which have multipliers inside the unit cycle by assumption of the stability of that resulting system, namely $-v/l_m$, which is always negative and

$$s(l_r, l_m)|_{l_m=l_r} = \mathscr{M}(\bar{e}_{1m}) - D. \tag{15}$$

The zero-crossing of the latter expression $\mathscr{M}(\bar{e}_{1m}) - D$ turns out to be the test-function for the transcritical bifurcation, TC. In these points the growth rate of the mutant population $\mathscr{M}(\bar{e}_{1m})$ equals just the depletion rate D. When the growth rate $\mathscr{M}(\bar{e}_{1m})$ is greater than the depletion rate D the equilibrium E_0 becomes unstable. As a result the mutant can invade. Hence the invasibility condition reads $\mathscr{M}(\bar{e}_{1m}) > D$.

Tilman (1982) discussed competition on the ecological time scale between two species modelled by the Monod–Herbert model in a chemostat with one nutrient. The so-called Tilman R^* rule says that the winner is the competitor that produces the lowest concentration of the nutrient at equilibrium in the absence of the competition. When (3) and (10) are substituted in (8c) we can derive that in equilibrium $df(\bar{x}_0)/dl|_{l=0} > 0$. We recall that in the limiting case $l = 0$ the two parameters m and g are infinite, but their quotient $v/g = \mu = I\eta_{V\mathscr{G}}/\eta_{X\mathscr{A}}$ is finite. This, in combination with the fact that the functional response is monotonously increasing, leads to the conclusion that $\bar{x}_0$ is minimal when $l = 0$. If our model follows the Tilman R^* rule, that is, the species without reserves should always win. In order to show this we analyse the stability of the system with a resident population without storage ($l = 0$), in which a mutant with storage ($l > 0$) tries to invade. For all mutants with $l > 0$ we have

$$\begin{aligned} \mu f(x_0^*)|_{l=0} - m &= \mathscr{M}(f(\bar{x}_0))|_{l=0} \\ &= D > \mathscr{M}(f(\bar{x}_0))|_{l>0} \\ &= \frac{\mu f(\bar{x}_0)|_{l=0} - m}{1 + \left(\dfrac{3m}{4\mu} + f(\bar{x}_0)\right)\eta_{V\mathscr{G}} l}. \end{aligned} \tag{16}$$

Observe that for both growth rates the same equilibrium $f(\bar{x}_0)$ is used since the resident population sets the environment as a result of the fact that the mutant is initially rare. We conclude that on the evolutionary time scale, under constant conditions in the chemostat a species without reserves is the evolutionary end-point. So, this system follows the pessimisation principle: mutation and natural selection leads to a deterioration of the environmental condition (Mylius and Diekmann, 1995; Diekmann, 2004).

4.2. Periodic environment

Now, we derive the mutant invasion fitness in a periodically fluctuating system. Numerical bifurcation analysis showed that for the nutrient and resident population the periodic orbit with period T_0 is stable for parameter values in the range of interest (see Fig. 1).

The stable periodic solution denoted by

$$L_0(t) = (\tilde{x}_0(t)\ \ \tilde{e}_{1r}(t)\ \ \tilde{x}_{1r}(t)\ \ \tilde{e}_{1m}(t)\ \ \tilde{x}_{1m}(t))^T, \tag{17}$$

will now be studied. The function $\tilde{e}_{1m}(t)$ is the solution of the linear ODE (11d) with a periodic coefficient $\tilde{f}(t)$

$$\frac{d\tilde{e}_{1m}}{dt} = \frac{\mu}{\eta_{V\mathscr{G}} l_m}(\tilde{f}(\tilde{x}_0(t)) - \tilde{e}_{1m}), \tag{18}$$

and a periodic boundary condition $\tilde{e}_{1m}(0) = \tilde{e}_{1m}(T_0)$. In order to study invasion of the mutant population into the resident population at $L_0(t)$ we have $\tilde{x}_{1m}(t) = 0$ and $\tilde{e}_{1m}(t) = \tilde{e}_{1r}(t)$, $t \in [0, T_0]$.

Let $\mathscr{I}(t)$ now be a 3×3 continuous periodic Jacobian matrix of period T_0 and $\Psi(t)$ the fundamental matrix of $\dot{y} = \mathscr{I}(t)y$, where

$$y(t) = \begin{pmatrix} x_0(t) - \tilde{x}_0(t) \\ e_{1r}(t) - \tilde{e}_{1r}(t) \\ x_{1r}(t) - \tilde{x}_{1r}(t) \end{pmatrix}. \tag{19}$$

The 5×5 periodic Jacobian matrix denoted by $\mathscr{J}(t)$ reads

$$\mathscr{J}(t) = \begin{pmatrix} & & 0 & -I\tilde{f}(t) \\ & \mathscr{I}(t) & 0 & 0 \\ & & 0 & 0 \\ 0 \quad 0 & \dfrac{\mu}{\eta_{V\mathscr{G}} l_m}\tilde{f}'(t) & \dfrac{\mu}{\eta_{V\mathscr{G}} l_m} & 0 \\ 0 \quad 0 & 0 & 0 & \tilde{\mathscr{M}}(t) - D \end{pmatrix}, \tag{20}$$

where $\tilde{f} = f(\tilde{x}_0)$, $\tilde{f}' = \frac{df}{dx_0}(\tilde{x}_0)$ and for the instantaneous actual growth rate of the mutant $\tilde{\mathscr{M}}(t) = \mathscr{M}(\tilde{e}_{1m}(t))$. Then with initial condition $\Phi(0) = I$ and where

$$z(t) = \begin{pmatrix} y(t) \\ e_{1m}(t) - \tilde{e}_{1m}(t) \\ x_{1m}(t) - \tilde{x}_{1m}(t) \end{pmatrix}, \tag{21}$$

the fundamental matrix $\Phi(t)$ of $\dot{z} = \mathscr{J}(t)z$ is given by

$$\Phi(t) = \begin{pmatrix} & & & 0 & \eta_1(t) \\ & \Psi(t) & & 0 & \eta_2(t) \\ & & & 0 & \eta_3(t) \\ \zeta_1(t) & \zeta_2(t) & \zeta_3(t) & \exp\left(-\dfrac{\mu t}{\eta_{V\mathscr{G}} l_m}\right) & \eta_4(t) \\ & 0 \quad 0 & & 0 & \exp\left(\int_0^t (\tilde{\mathscr{M}} - D)\, d\tau\right) \end{pmatrix}. \tag{22}$$

All functions are evaluated along the periodic orbit L_0.

Any solution $z(t)$ satisfies

$$z(T_0) = \Phi(T_0)z(0). \tag{23}$$

In the region below the TC curve in Fig. 1 the periodic orbit of the nutrient and residents population system on the periodic solution L_0 is stable and there is one eigenvalue of the matrix $\Psi(T_0)$ is equal to 1 and the other 2 eigenvalues are inside the unit cycle. Expanding the determinant of the

monodromy matrix $\Phi(T_0)$ evaluated at the cycle L_0

$$\det(\Phi(T_0)-\mu_1 I) = \det(\Psi(T_0)-\mu_1 I) \times (e^{-\frac{\mu T_0}{\eta V \mathscr{G} l_m}}-\mu_1) \times (e^{\int_0^{T_0}\tilde{\mathscr{M}}(t)\,dt - T_0 D}-\mu_1), \quad (24)$$

we find that besides the three eigenvalues of $\Psi(T_0)$ there are two additional Floquet multipliers, eigenvalues of $\Phi(T_0)$, namely $\exp(-\frac{\mu T_0}{\eta V \mathscr{G} l_m})$, which lies always inside the unit circle, and $\exp\left(\int_0^{T_0}\tilde{\mathscr{M}}(t)\,dt - T_0 D\right)$. When under parameter variation this second multiplier μ_1 crosses the unit circle, the cycle L_0 changes stability. The trait value where the dominant Floquet multiplier equals one, $\mu_1 = 1$, indicates a transcritical bifurcation for the periodic solution. Generally this means a change of the invasibility of the resident population(s) by the mutant when the trait value is varied. That is, the invasibility condition $s = \log(\mu_1)$ reads

$$s(l_r, l_m)|_{l_m=l_r} = T_0^{-1}\int_0^{T_0}\tilde{\mathscr{M}}(t)\,dt - D > 0. \quad (25)$$

When $\mu_1 = 1$ and consequently $s = 0$, the mean growth rate of mutant population equals just the depletion rate D.

5. Evolutionary course of the nutrient-population system

In this section we study the invasion of a mutant in a monomorphic population. The reference parameter values are given in Table 1. Because the nutrient inflow is periodic an ecologically stable dimorphic population is possible. Therefore, we also study the evolutionary stability of the resulting dimorphic population.

5.1. Invasion of the monomorphic population

The pairwise invasibility plot (PIP) (Geritz et al., 1998) for $\varepsilon = 1$ is given in Fig. 2. At the diagonal the mutant equals the resident and the model for the nutrient, resident population and mutant population has no unique solution. That is each point on the diagonal is a structurally unstable bifurcation point, that is, when the mutant possesses the same trait value of as the resident their biomasses are not fixed, only the sum of both biomasses in order to fulfil mass conservation. A similar bifurcation point was found in Kooi and Kooijman (2000) where the effects were studied of predation of two prey populations competing for a single nutrient in a chemostat environment.

The parameter space (l_r, l_m) is divided in three different regions: '+'-the mutant can invade and replaces the resident, '−'-the mutant cannot invade and goes extinct, '++'-the mutant can invade but cannot replace the resident which leads to coexistence (see Fig. 3). We calculated the periodic solution biomasses of the resident and mutant populations together with the nutrient in the chemostat of ecosystem (11) using AUTO (Doedel et al., 1997) where l_m is varied such that $l_r = l_m + 0.3$. Fig. 3 shows the minimum and maximum of these periodic solution biomasses. There are five regions for the l_m value with different long-term dynamics of the ecological system. In the regions **a** and **e** the mutant persists and the resident population goes extinct. In region **c** the mutant population goes extinct and the resident persists. There is coexistence in the regions **b** and **d**. These regions are separated by transcritical bifurcation points where the dominant multiplier equals 1.

These transcritical bifurcations form the boundaries of the area of coexistence (AOC) in Fig. 2 denoted by TC^+ and

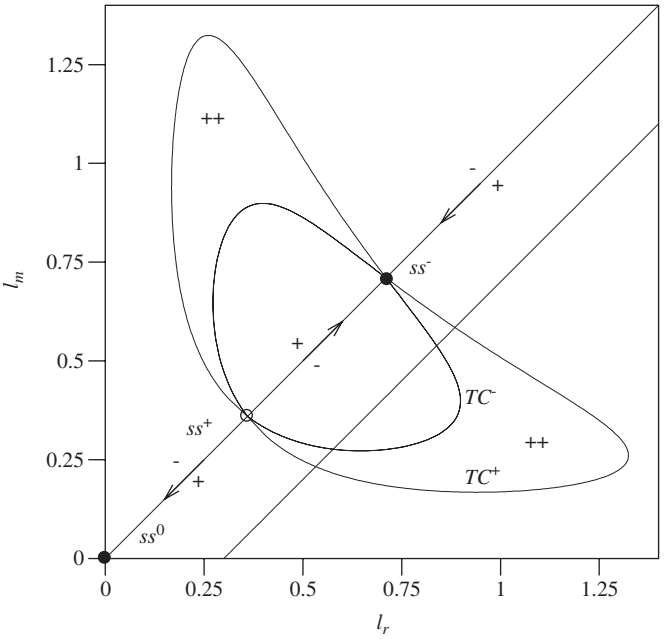

Fig. 2. Pairwise invasibility plot (PIP) Geritz et al. (1998)-plot: '+'-mutant may invade and replace the resident, '−'-mutant cannot invade, '++' mutant can invade but not replace the resident (mutual invasibility leading to coexistence). There are two singular points ss^- and ss^+. The origin ss^0 is a population without energy storage, it is reachable and an evolutionary end-point.

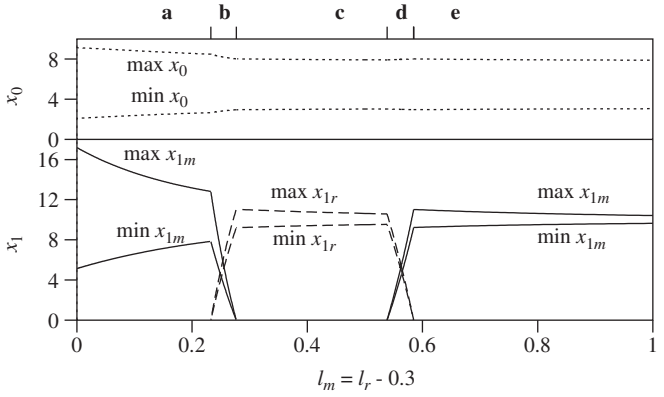

Fig. 3. Maximum and minimum nutrient concentration x_0 and biomasses x_1 of resident and mutant as function of the traits $l_m = l_r - 0.3$ for the monomorphic resident population where $\varepsilon = 1$. These curves were calculated with AUTO (Doedel et al., 1997). In region **c** the resident with l_r persists while in regions **a** and **e** the mutant invades and replaces the resident, so the trait value equals l_m. In **b** and **d** there is coexistence.

TC^- where both mutant and resident coexist with positive biomass (see also Fig. 3). At these curves both the maximum and minimum biomass during one period of the resident or mutant population is zero and therefore these curves are also zero contour lines. The transcritical bifurcation curves meet in two points at the diagonal. These points are singular strategies, ss's, where the invasion gradient is zero

$$\left.\frac{\partial s(l_r,l_m)}{\partial l_m}\right|_{l_m=l_r}=0. \tag{26}$$

These points are equilibrium points of the canonical equation (12).

Fig. 4 shows the invasion fitness of the mutant population invading the resident population at the two singular points ss^- and ss^+ where the invasion gradient vanishes. Both curves $s(l_r=l_r^*,l_m)$ where l_m is varied, and $s(l_r,l_m=l_r^*)$ where l_r is varied, are plotted.

In Geritz et al. (1998) eight different singular strategies are distinguished based on the second derivatives at the point. It appears that the slope of the non-trivial zero contour line by a ss determines for the monomorthoc population already the evolutionary dynamics in the neighbourhood of the ss. Hence, the curves in Fig. 4 show that ss^- (solid line) is evolutionary stable and ss^+ (dashed line) is evolutionary unstable (compare Geritz et al., 1998, Fig. 4 case (a) and (d)). When l_r^* is changed for its ss^--value to its ss^+-value the invasion fitness curves change smoothly for the solid curves into the dashed curves showing the influence of the feedback via the nutrient dynamics. Similar plots for point ss^0 shows that in this point the invasion gradients are not zero, its a boundary optimum.

At point ss^- we have

$$\left.\frac{\partial^2 s(l_r,l_m)}{\partial l_m^2}\right|_{l_m=l_r}<0,\quad \left.\frac{\partial^2 s(l_r,l_m)}{\partial l_r^2}\right|_{l_m=l_r}>0,$$
$$\left.\frac{\partial^2 s(l_r,l_m)}{\partial l_r^2}\right|_{l_m=l_r}-\left.\frac{\partial^2 s(l_r,l_m)}{\partial l_m^2}\right|_{l_m=l_r}>0,$$

which means that ss^- is evolutionarily stable and convergence stable, and therefore a continuously-stable strategy CSS. At point ss^+ we have

$$\left.\frac{\partial^2 s(l_r,l_m)}{\partial l_m^2}\right|_{l_m=l_r}>0,\quad \left.\frac{\partial^2 s(l_r,l_m)}{\partial l_r^2}\right|_{l_m=l_r}<0,$$
$$\left.\frac{\partial^2 s(l_r,l_m)}{\partial l_m^2}\right|_{l_m=l_r}+\left.\frac{\partial^2 s(l_r,l_m)}{\partial l_r^2}\right|_{l_m=l_r}>0,$$

and therefore point ss^+ is evolutionarily unstable and convergence unstable.

5.2. Invasion of the dimorphic population

When the mutant does not replace the resident, but the two coexist, a dimorphic resident population is formed. To investigate the evolutionary fate of such a dimorphic system, we study the situation where a mutant tries again to invade it. The invasion fitness gradient given by $s(l_{r1},l_{r2},l_m)$ (25) is now derived for the stable periodic solution of the seven-dimensional system

$$L_0(t)=(\tilde{x}_0(t)\ \tilde{e}_{1r1}(t)\ \tilde{x}_{1r1}(t)\ \tilde{e}_{1r2}(t)\ \tilde{x}_{1r2}(t)\ \tilde{e}_{1m}(t)\ \tilde{x}_{1m}(t))^T. \tag{27}$$

The evolutionary course is again described by (13).

The results are depicted in Fig. 5. In addition to the transcritical bifurcation curves TC^+ and TC^-, which form the boundaries of the (AOC) two curves appear where the invasion gradient of the mutant invading the dimorphic system vanishes

$$\left.\frac{\partial s(l_{r1},l_{r2},l_m)}{\partial l_m}\right|_{l_m=l_{ri}}=0,\quad i=1,2. \tag{28}$$

These curves, denoted by Z^- and Z^+, are zero-isoclines of the canonical Eq. (13).

In Fig. 6 the AOC of the two residents in the three-dimensional parameter space (l_{r1},l_{r2},l_m) is drawn. For each pair (l_{r1},l_{r2}) the biomasses and energy densities for the dimorphic population are fixed by the ecosystem dynamics,

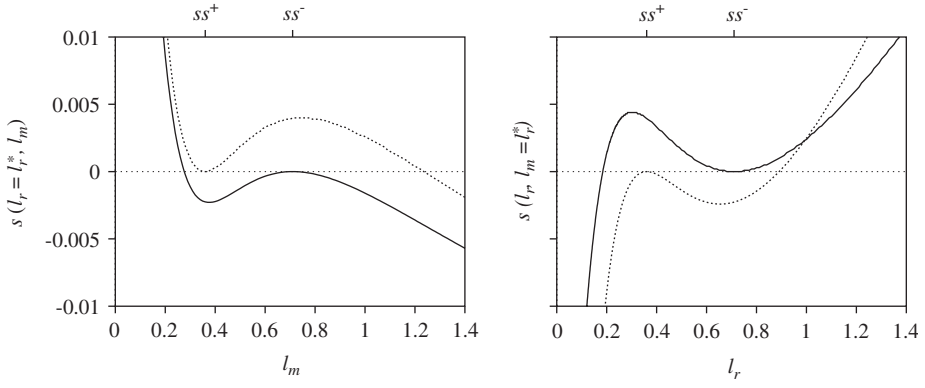

Fig. 4. The invasion fitness of a mutant invading the resident at the two singular strategies ss^- and ss^+ where $\frac{\partial s(l_r,l_m)}{\partial l_m}|_{l_m=l_r=l_r^*}=0$. On the left the fitness $s(l_r,l_m)|l_r=l_r^*$ is shown for a range of mutants, on the right $s(l_r,l_m)|l_m=l_r^*$ for a range of residents. The solid line is for singular strategy ss^- and the dotted curve for ss^+.

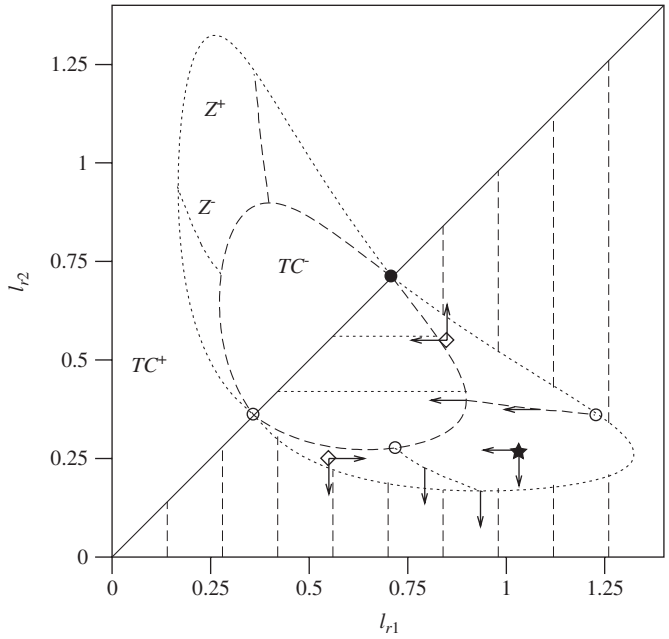

Fig. 5. Bifurcation diagram for the dimorphic population. At the two curves the invasion gradient is zero. The horizontal arrows of the invasion cones are related to invasion of progenitor resident with trait value l_{r1} ($>l_{r2}$) and the vertical arrows with l_{r2} ($<l_{r1}$).

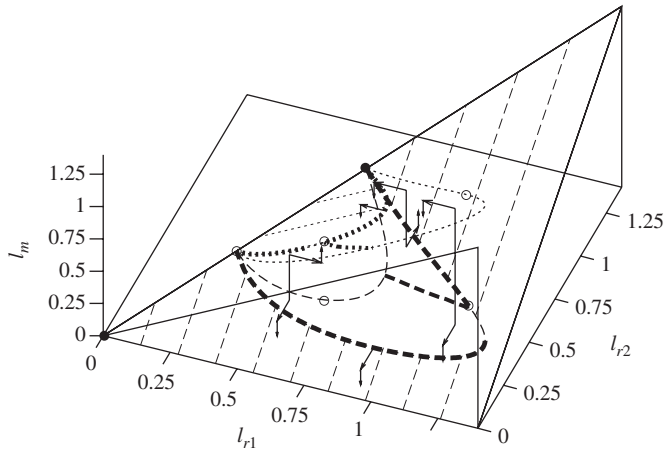

Fig. 6. Three-dimensional PIP plot for the dimorphic resident population. Evolutionary changes of the resident with trait l_{r1} take place in the top plane and those due to changes of the resident with trait l_{r2} in the bottom plane. The bullet and open circle on the diagonal indicate the singular strategies of the monomorphic population. The circles on the transcritical bifurcations mark evolutionary steady states. An evolutionary path can leave the AOC via the parts of its boundary indicated by thick lines. At these point the mutant replaces its progenitor resident population and at the same time the non-progenitor resident goes extinct.

the solution of (11). These results $\tilde{x}_0(t), \tilde{e}_{1r}(t), \tilde{x}_{1r}(t)$ are independent of l_m (the vertical axis in Fig. 6) since $\tilde{x}_{1m}(t)=0$ and $\tilde{e}_{1m}(t)$ is calculated by solving the periodic ODE (18) where $\tilde{f}(t)$ is fixed by (5) and $\tilde{x}_0(t)$.

For one plane we have $l_m=l_{r1}$ where l_{r2} is free (for invasion of a mutant of the progenitor resident with largest trait value), and the other where $l_m=l_{r2}$ and l_{r1} is free. These two subdiagonal planes intersect at the diagonal line $l_m=l_{r1}=l_{r2}$ to which the monomorphic dynamics are restricted. The points $l_{r1}=l_{r2}=l_m$ where the invasion gradient is zero, (26), indicated by filled and open circles are again singular strategies for the monomorphic population.

The arrows in Fig. 6 correspond to those in Fig. 5, and indicate for each region the directions of the evolutionary change, the so called 'invasion cone' (Matessi and Di Pasquale, 1996). These evolutionary changes are explained graphically in Figs. 7 and 8.

Now we derive the evolution course starting in the three regions of the AOC separated by the isoclines $Z^{\pm}$ and the boundary curves of the AOC formed by the $TC^{\pm}$. In order to study evolution close to the two singular strategy points of the monomorphic population we consider invasion of the dimorphic population for points in the neighbourhood of these points where the two resident populations can coexist. These two points are indicated by diamonds in Fig. 5.

The invasion fitness of a mutant invading two coexisting residents with $l_{r1}=0.85, l_{r2}=0.55$ (left) and $l_{r1}=0.55, l_{r2}=0.25$ (right) is shown in Fig. 7. We recall that for values of l_m the biomasses $\tilde{x}_{1ri}(t)$ and energy reserves $\tilde{e}_{1ri}(t)$, $i=1,2$ are fixed by the stable periodic solution of the ecological system (27). In the first point the curve of the mutant's invasion fitness in the dimorphic population is a parabola as shown in Geritz et al. (1998, Fig. 2 case (c) and Fig. 4 case (b)). For $l_{r1}<l_m<l_{r2}$, invasion leads to replacement of its progenitor resident by the mutant. For $l_m<l_{r1}$ or $l_m>l_{r2}$ the residents are uninvasible. Thus, there is convergence toward the singular strategy ss^-. Observe that the direction of the arrows correspond to the direction of the arrows of the invasion cones belonging to the point studied close to diagonal in Fig. 5.

In the second point close to point ss^+ in Fig. 7 (right) for $l_{r1}<l_m<l_{r2}$, both residents are uninvasible. With $l_m<l_{r1}$ or $l_m>l_{r2}$, however, invasion leads to replacement of its progenitor resident by the mutant and we have disruptive selection similar to Geritz et al. (1998, Fig. 4 case (e) and Fig. 2 case (h)). That is, point ss^+ is evolutionarily and convergence unstable.

Observe that in two intervals the dominant multiplier is constant. In these regions multiplier other than the one associated with the invasion of the mutant, the term $\exp\left(\int_0^{T_0}\tilde{\mathscr{M}}(t)\,dt - T_0 D\right)$ in (24), is dominant. This multiplier, a root of $\det(\Psi(T_0)-\mu_1 I)$ in (24), is independent of the trait value l_m and equals 1 when one of the resident population has a trait value on the transcritical bifurcation curve. As a result, close to the boundary of the AOC, the bifurcation curves TC, the difference between the two largest multipliers can be very small. This difference can be enlarged by taking the average over many cycles (say 10 or 100) instead of 1 cycle for the calculation of the invasion fitness.

Fig. 8 gives the invasion fitness $s(l_{r1}, l_{r2}, l_m)$ of a mutant invading two coexisting resident in a third point in the trait

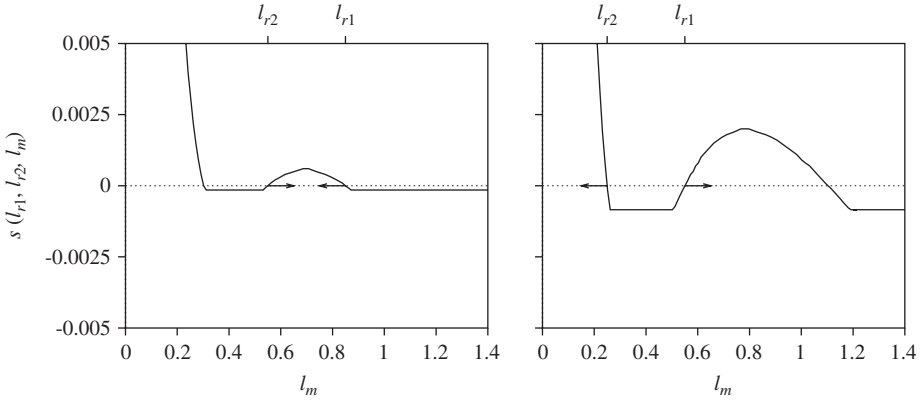

Fig. 7. The invasion fitness of a mutant invading two coexisting resident with $\varepsilon = 1$ and $l_{r1} = 0.85, l_{r2} = 0.55$ (left) and $l_{r1} = 0.55, l_{r2} = 0.25$ (right). See Fig. 5 for the position, indicated by the diamonds, of the points in the two-dimensional trait space.

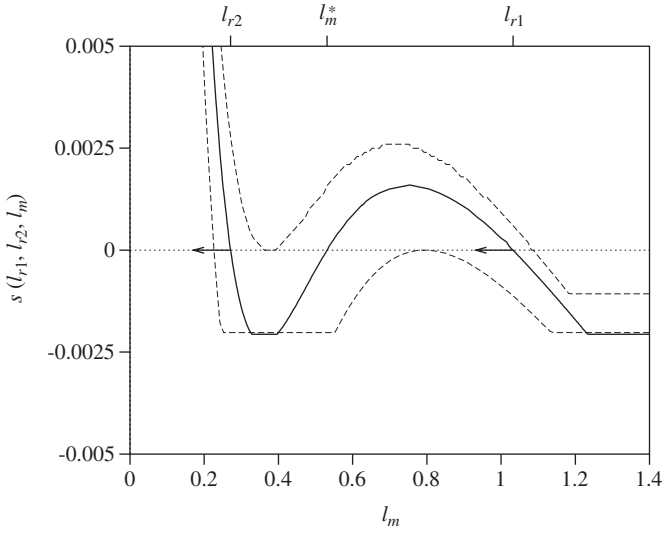

Fig. 8. The invasion fitness of a mutant invading two coexisting resident with $\varepsilon = 1$, $l_{r1} = 1.032128$ and $l_{r2} = 0.271164$. See Fig. 5 for the position of the point in the two-dimensional trait space indicated by a star. At $l_m^* = 0.531168$ the system has one multiplier equal to 1. The top dashed line is for a point on the Z^+-curve: $l_{r1} = 1.086426, l_{r2} = 0.374409$ and the bottom dashed line is for a point on the Z^--curve: $l_{r1} = 0.793414, l_{r2} = 0.226464$.

space, $l_{r2} = 0.271164$ and $l_{r1} = 1.032128$ in the region bounded by the two isoclines $Z^{\pm}$ (see Fig. 5 where the point is indicated by a star). At $l_m^* = 0.531168$ the invasion fitness of the system is zero. For $l_m < l_{r2}$ invasion leads to replacement of the resident with trait value l_{r2}, for $l_{r2} < l_m < l_m^*$ the residents are uninvasible, for $l_m^* < l_m < l_{r1}$ the mutant replaces the resident with trait value l_{r1} and finally for $l_{r1} < l_m$ the residents are uninvasible. For our purpose only l_m values close to the resident trait values l_{r1} and l_{r2} are important since we are interested in small evolutionary steps. The arrows in Fig. 8 show that invasion of both residents leads to replacement by a mutant with a smaller trait value, and this explains the direction of the arrows of the invasion cone in Fig. 5 for the point in the region of the AOC bounded by the two isoclines $Z^{\pm}$ and indicated by a star.

The curve of the mutant's fitness in the dimorphic population with traits l_{r1} and l_{r2} is not a parabola as shown in Fig. 7 but like a cubic polynomial. This point is degenerated since at this point ecosystem (11) has no unique solution. For $l_{r2} < l_m < l_m^*$ we have $x_{1r2} > 0$, $x_{1r1} > 0$ and $x_{1m} = 0$ but in the interval $l_m^* < l_m < l_{r1}$ we have $x_{1r2} = 0$, $x_{1r1} > 0$ and $x_{1m} > 0$. The solution for $x_{1r2} = 0$ and $x_{1m} = 0$ switches discontinuously at the critical point $l_m^* = 0.531168$. Similar to the monomorphic case where the mutant trait value equals the resident trait value on the diagonal in the PIP plot, this point is structurally unstable, that is, when a mutant possesses the same trait value as one of the residents their biomasses are not fixed, only their sum.

The invasion fitness of a mutant invading two coexisting residents and $l_{r1} = 1.086426$, $l_{r2} = 0.374409$ and $l_{r1} = 0.793414$, $l_{r2} = 0.226464$ both on a zero fitness gradient curve $Z^{\pm}$, is also shown in Fig. 8. case we have for the invasion gradient $\partial s(l_{r1}^*, l_m)/\partial l_m = 0$. With $l_m < l_{r2}$ invasion leads to replacement of the resident and for $l_{r2} < l_m$ the residents are uninvasible. In the second case also the invasion gradient is also zero at the trait value of the progenitor resident, but now for $l_m = l_{r2}$ there is replacement of the resident with trait value l_{r1}.

A convergence equilibrium of the dimorphic system is given by an intersection point of the isoclines Z^+ and Z^- where both right-hand sides of the canonical equations (13) are zero simultaneously. Fig. 5 shows that there is no intersection point and therefore there is no evolutionary singular coalition (Metz et al., 1996; Geritz et al., 1997, 1998, 1999).

We now derive properties of the isoclines (where they terminate). The curve Z^- (in the lower diagonal) terminates on the curve TC^+ where l_{r2} is minimum, denoted in Fig. 9 by t^{--}. This can be seen as follows. On that curve we have $x_{1r1} = 0$. Since, by assumption, the mutant population is rare we also have $x_{1m} = 0$. For the progenitor resident population we have $x_{1r2} > 0$. Hence, we have $l_m = l_{r1}$ and also $x_{1r1} = x_{1m} = 0$, and therefore with respect to invasion of the progenitor resident population with trait

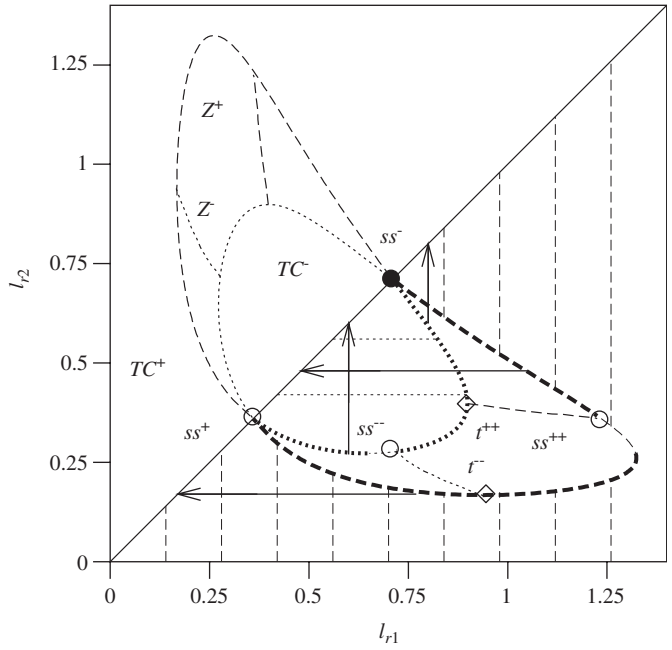

Fig. 9. State space for the canonical equations (13) for the dimorphic population. The solid circles (ss^-, ss^0) and open circle (ss^+) on the diagonal are evolutionary steady states for the monomorphic population and the two open circles at the boundary of coexistence those for the dimorphic population, the curve TC. The thick lines as part of the boundary of the AOC mark intervals where the evolutionary path can leave that region. At those points only one resident population survives and the system becomes monomorphic again. The horizontal lines indicate the transition at which the resident with the largest trait value went extinct and the vertical lines those with the smallest trait value.

l_{r2} the other resident and the mutant are interchangeable. Along the curve TC^+ we have $s(l_{r1}, l_{r2}) = 0$; one multiplier of the monodromy matrix $\Phi(T_0)$ equals 1. Because the determinant of the matrix can be written with two linear factors in (24) we have also $s(l_{r1}, l_{r2}, l_m)|_{l_{r1}=l_m} = 0$. Since the line tangent to TC^+ is horizontal, at the point of interest we have $\partial s(l_{r1}, l_{r2}, l_m)/\partial l_{r1}|_{l_{r1}=l_m} = 0$ and consequently at that point also $\partial s(l_{r1}, l_{r2}, l_m)/\partial l_m|_{l_m=l_{r1}} = 0$. Fig. 6 shows that this same ecological system point (l_{r1}, l_{r2}) is invasible by a mutant with $l_m = l_{r2}$ and therefore this point is not an evolutionary singular point in the resident trait space.

The curve Z^- intersects the curve TC^- also in a special point. Namely at the point denoted by ss^{--} in Fig. 9 where the trait value l_{r1} equals that of the point ss^-. For in point ss^{--} on the curve TC^- we have $x_{1r2} = 0$ and furthermore $s(l_{r1}, l_{r2}) = 0$. Since the biomass x_{1r2} is zero the structure of the fundamental matrix $\Phi(t)$ for this nutrient–two-resident five-dimensional system $\tilde{x}_0(t), \tilde{e}_{1r1}(t), \tilde{x}_{1r1}(t), \tilde{e}_{1r2}(t), \tilde{x}_{1r2}(t)$ equals that of (22). Invasion of this system by a mutant population extends the system to a seven-dimensional system where the nutrient–two-resident five-dimensional system becomes the $\Psi(t)$ submatrix. Thus the invasion rate of the mutant population into the dimorphic system at point ss^{--} equals the invasion rate into the monomorphic system at point ss^- for all trait values l_m. In point ss^- we have for the invasion gradient for the monomorphic population $\partial s(l_{r1}, l_{r2})/\partial l_{r2}|_{l_{r2}=l_{r1}} = 0$ where the second resident plays the role of the mutant, and consequently for the dimorphic population at point ss^{--} also $\partial s(l_{r1}, l_{r2}, l_m)/\partial l_m|_{l_m=l_{r1}} = 0$, that is, its a point on the curve Z^-.

Similar properties can be derived for Z^+ that terminates on the curve TC^- where $x_{1r2} = 0$, namely at the point where l_{r1} is maximum, denoted in Fig. 9 by t^{++}. That is, where the tangent to the TC^- curve is vertical. Then $\partial s(l_{r1}, l_{r2}, l_m)/\partial l_{r2}|_{l_{r2}=l_m} = 0$ leads to $\partial s(l_{r1}, l_{r2}, l_m)/\partial l_m|_{l_m=l_{r2}} = 0$ at that point. On the other end, curve Z^+ terminates on the curve TC^+ where $x_{1r1} = 0$ denoted by ss^{++}, with trait l_{r2} equal to that of the point ss^+, that is both points are on an horizontal line.

Evolutionary paths leave the AOC via the parts of its boundary indicated in Fig. 9 by thick lines. At these points the mutant replaces its progenitor resident population and at the same time the other resident goes extinct. Thereafter, the diagram Fig. 2 for the monomorphic population is valid. The point on the diagonal where evolution continues depends on where the evolutionary path crosses the boundary of AOC. The direction of the arrows in Fig. 9 indicating where on the diagonal evolution continues can be derived from Fig. 3. When the path crosses the boundary along the curve TC^- the resident with the largest trait value remains and therefore the point on the diagonal where the monomorphic population continues is above the place of crossing. On the other hand when it leaves the curve TC^+ the monomorphic population with the smallest trait value survives and evolution continues in a point on the diagonal to the left with respect to the point of crossing (see Fig. 9). So, there can be convergence to the stable ss^- or to ss^0 where the remaining population looses its storage at $l = 0$.

There is always convergence to the stable ss^- when the evolutionary path leaves the AOC via curve TC^- (a small part close to ss^{--} is not reachable). The curve TC^+ is split into two intervals. Between the monomorphic singular strategy point ss^- and the evolutionary dimorphic singular strategy point ss^{++}, gives also convergence to ss^-. Between ss^{++} and ss^+ (part is not reachable) the evolutionary course continues on the diagonal below point ss^+ and therefore leads to a monomorphic population without reserves.

We conclude that there is protected dimorphism, that is, the resident and mutant population can invade each other at the ecological time scale, but there is no evolutionarily singular coalition at the evolutionary time scale. Therefore depending on the initial evolutionary state there is convergence to the monomorphic stable ss^- with $l > 0$ or to the monomorphic strategy without energy storage ss^0 where $l = 0$. These results agree with the classification of the singular strategies given in Geritz et al. (1998) but also hold for large mutational steps.

6. Effects of the amplitude of the forcing function

Now we take the amplitude of the forcing function, ε, as a bifurcation parameter. We recall that for $\varepsilon = 0$ the system

is autonomous and no mutant population can coexist with the resident population because of competitive exclusion. The PIP plots for $\varepsilon = 0.867$, 0.8653, 0.86 and 0.85258 are given in Fig. 10.

With $\varepsilon = 0.867$ the plot shown in Fig. 11 resembles the plot for $\varepsilon = 1$ shown in Fig. 5, now the two singular strategies indicated by ss^- and ss^+ are close to each other. However, the evolutionary stability of ss^- has changed and has become an evolutionarily branching point (EBP) Geritz et al. (1998, Fig. 2 case (b)). Hence ss^- is still convergence stable but not evolutionary stable (in Fig. 11 it is now indicated by an open circle). As a result, disruptive selection induces the difference in the trait values of the two coexisting strategies to grow. Protected dimorphism exists, however, in the AOC on the left-hand side of the zero invasion gradient curve Z^- adjacent to the two singular points ss^- and ss^+, the invasion gradients have the same sign and all evolutionary paths leave the AOC via a bottom part of its boundary where a resident goes extinct. Evolution stops at point ss^0.

This pattern is similar to that found in Geritz et al. (1999, Fig. 12). In Dercole (2003) evolutionary cycles occur, but here the evolutionary path leaves the AOC via the lower boundary, the curve TC^-, where the resident with

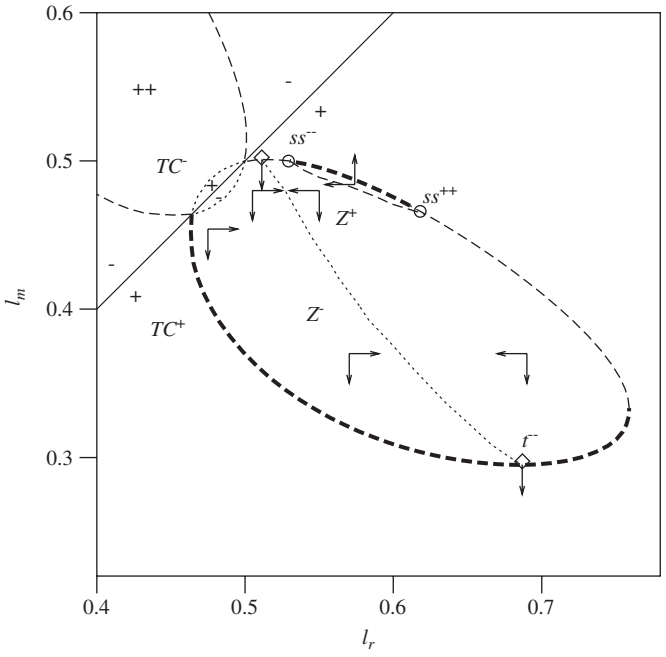

Fig. 11. PIP-plot with $\varepsilon = 0.867$: '+'-mutant can invade and replace the resident, '−'-mutant cannot invade, '++' mutant may invade but cannot replace the resident (mutual invasibility resulting in coexistence).

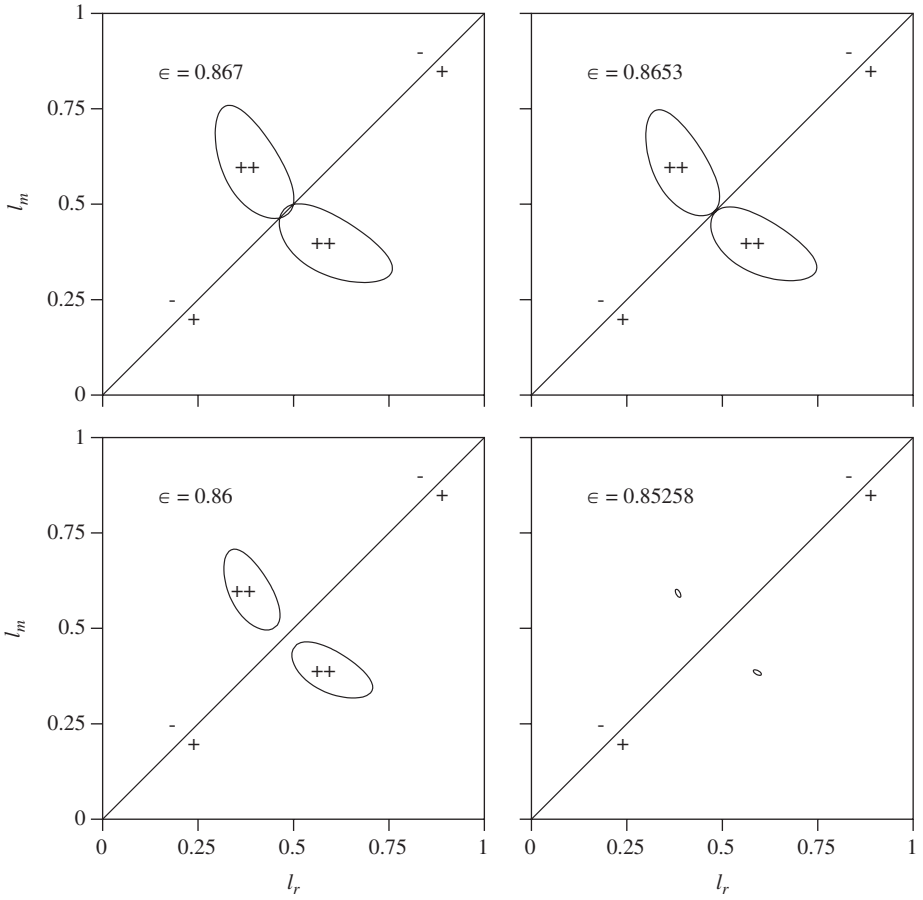

Fig. 10. PIP-plot with instead of $\varepsilon = 1$:$\varepsilon = 0.867$, $\varepsilon = 0.8653$ $\varepsilon = 0.86$ and $\varepsilon = 0.85258$: '+'-mutant may invade and replace the resident, '−'-mutant cannot invade, '++' mutant may invade but cannot replace the resident (mutual invasibility resulting in coexistence). At about $\varepsilon = 0.8525$ the isola's disappear.

the largest trait value goes extinct, and evolution continues as a monomorphic species.

Comparing the bifurcation diagrams for $\varepsilon = 0.867$ with $\varepsilon = 1$, reveals that at an intermediate value, point ss^- becomes unstable. This critical point is denoted by Z and the value of the amplitude ε_Z. At that point the boundary of the AOC, the transcritical bifurcation curves intersects ss^+ horizontally (TC^+) and vertically (TC^-). Both zero invasion gradient curves Z^+ and Z^- terminate at $ss^{--} = ss^-$. Lowering ε at the critical point Z, both ss^{++} and ss^{--} are on the same transcritical bifurcation curve TC^+. Starting above Z^- evolution goes towards the adjacent transcritical curve and the remaining monomorphic population possesses a trait value between ss^+ and ss^- on the diagonal (see also Fig. 9), and evolution continues as a monomorphic species.

Lowering ε further, for $\varepsilon = \varepsilon_T = 0.8653$ the boundaries of the AOC touch at the diagonal where the two points ss^- and ss^+ collide and disappear while the same holds for ss^{--} and ss^{++} and the isocline curve Z^+. This phenomenon resembles what happens when a stable and unstable periodic solution collide at the tangent or saddle-node bifurcation point for a periodic solution of a nonlinear autonomous dynamical system. Therefore, this critical point is denoted by T (from "tangent" bifurcation).

For values of ε less than $\varepsilon = \varepsilon_T$ two isolated regions exist where mutants could invade, leading to two coexisting populations. These regions are, however, unreachable for monomorphic residents by small mutational steps. Finally for $\varepsilon < 0.8525$ the isola's disappear.

We conclude that for all amplitudes ε the evolutionary end-point is a monomorphic population. Fig. 12 is a one-parameter bifurcation diagram with the amplitude as bifurcation parameter. For $\varepsilon = 1$ the inflow of nutrient is always positive, $\varepsilon = 1$ the minimum nutrient concentration in the inflow during the cycle is precisely zero and for $\varepsilon > 1$ the periodic inflow has a positive cut-off sinusoidal shape.

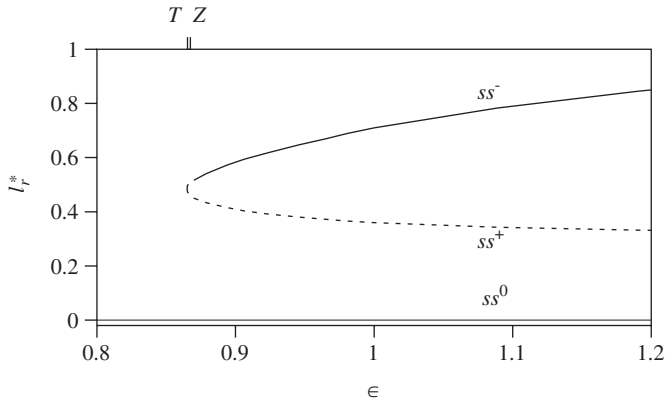

Fig. 12. Bifurcation diagram for the canonical equations with ε as free parameter. There is bi-stability (ss^- and ss^0) for $\varepsilon > \varepsilon_Z$. For $\varepsilon < \varepsilon_Z$ the singular strategy ss^0 is the unique stable ss. At the tangent bifurcation point T both ss^{++} and ss^{--} disappear simultaneously. Below T ss ss^0 is the unique evolutionary end-point.

The trait value for the singular strategy points l_r^* are plotted as a function of ε. For amplitudes smaller than the bifurcation point Z where ss^- becomes convergence unstable ($\varepsilon < \varepsilon_Z$) the end-point is a monomorphic population without storage, point ss^0 where $l = 0$. Consequently, a population without energy reserves, is the unique evolutionary end-point. For values $\varepsilon > \varepsilon_Z$ there is bi-stability and the monomorphic end-point depends on the evolutionary initial point $l_r(\tau = 0)$; there is convergence to either ss^+ or ss^0. We recall that by lowering ε, the singular strategy ss^- becomes evolutionary unstable while still convergence stable, at a higher trait value of the tangent bifurcation T where $ss^- = ss^+$ at which point the system looses convergence stability.

7. Discussion and conclusions

Shertzer and Ellner (2002) analysed a similar algae-rotifer model in order to study evolution of energy storage. Their model predicts that energy storage is a physiological mechanism for the stabilization of population dynamics. In this paper the periodic behaviour of the population originates entirely from the external periodic forcing and therefore these effects cannot be found. These differences arise from the differences in reserve dynamics.

The dynamics of the energy reserves introduced in Kooijman (2000) are based on physiological processes. Their dynamics are described by an additional ODE that models first order kinetics, not in the amount of energy, but in the energy density (which is the amount of energy divided by the structural biomass). This is different from reserves stored for later use via switches as a behavioural response to changing nutrient availability, as is how reserves are modeled by Shertzer and Ellner (2002).

Complexity is introduced here by the new first-order ODE for the dynamics of the energy density. Mathematically, a singular perturbation technique justifies the smooth transition of system (7) into (11) when $l \downarrow 0$. Therefore no extra parameters and switches are needed like in Shertzer and Ellner (2002).

The result that for all points in the parameter space the system has a periodic solution with period equal to the forcing period, is expected for a single population (the rotifer and non-vital algae) in the chemostat. In Kot et al. (1992) and Gragnani and Rinaldi (1995) it is shown that this does not hold true for food chains in a periodic environment, in general.

Invasion criteria of mutants into resident populations with periodic solutions that are due to external forcing, are similar to those for invasion of resident populations with periodic solutions when the resident species and the nutrient are part of an ecosystem with a non-equilibrium periodic attractor, as for example in Shertzer and Ellner (2002).

In this paper the PIP plot (Fig. 2) for the mutant population that tries to invade the resident population in the monomorphic population case is also considered a

bifurcation diagram (Fig. 5) of two resident population of the dimorphic population case and finally as the phase plane diagram (Fig. 9) for the evolutionary system. Observe that a complete bifurcation analysis including the dimorphic case of which the results are presented in Fig. 5 is not necessary when small mutational steps are assumed. Then the classification presented in Geritz et al. (1998) suffices to conclude that for the reference case with $\varepsilon = 1$, point ss^- is a continuously-stable strategy CSS. With $\varepsilon = 0.867$, point ss^- in Fig. 11 is an EBP and then even for small mutational steps an analysis including the dimorphic (and possibly polymorphic) case is required to follow the evolutionary process after branching.

Although Fig. 12 looks like an ordinary bifurcation diagram for continuous-time ODE-systems like the canonical equations, the bifurcation points are fixed by non-classical test functions where the equilibrium or non-equilibrium solutions of the ecological system play an important role. When the trait value of the mutant population equals that of a resident population, the ecological system are structurally unstable where the biomasses of the populations not fixed, only their sum. Furthermore this bifurcation diagram shows, in agreement with Geritz et al. (1999), that two independent stability concepts are involved, that is, evolutionary stability (on the right side of point Z) and convergence stability (on the right side of point T).

The resulting evolutionary dynamics and the dependence of a bifurcation parameter are very similar to those obtained in Geritz et al. (1999) of a seed size and seedling competitive ability. The plant population consists of a number of different plant types, each with its own seed size. Their model is not a continuous-time (mathematically described by a system of ODE's), but a discrete-time model (mathematically described by a system of difference equations or a map). The equilibrium condition is that the expected per capita number of established offspring is equal to one for all types. Invasion fitness for the mutant is the per capita number of their established offspring. In our case the periodic solution is fixed by a boundary value problem for the ODE's and the fitness is the mean (25) growth rate of mutant population. We refer to Boldin (2006) for a general description of biological invasion in Ecology, Adaptive Dynamics and Epidemiology.

In order to perform a numerical bifurcation analysis we have to make choices for the parameter values. We found that the obtained results are robust for a certain range around this parameter set. However, we cannot exclude the possibility that for parameter values far from those used here, the model predicts other evolutionary dynamics.

In a constant environment coexistence of two different populations is impossible, a phenomenon referred to as competitive exclusion which holds also for the model with reserves as was shown above. In a series of papers (Huisman and Weissing, 1999, 2001, 2002) it is shown that non-equilibrium dynamics allow the coexistence of many species on a few limiting resources and therefore may provide a potential explanation for the biodiversity of many communities. For our simple ecosystem, however, the evolutionary end-point is again a monomorphic population. This suggests that when evolutionary processes are taken into account in the long run non-equilibrium dynamics does not need to enhance biodiversity.

Acknowledgements

The authors would like to thank four anonymous reviewers for their valuable comments that helped to improve this paper.

References

Boldin, B., 2006. Introducing a population into a steady community: the critical case, the center manifold, and the direction of bifurcation. SIAM J. Appl. Math. 66 (4), 1424–1453.

Dercole, F., 2003. Remarks on branching-extinction evolutionary cycles. J. Math. Biol. 47 (6), 569–580.

Dercole, F., Irisson, J.-O., Rinaldi, S., 2003. Bifurcation analysis of a prey–predator coevolution model. SIAM J. Appl. Math. 63 (4), 1378–1391.

Diekmann, O., 2004. A beginners guide to adaptive dynamics. In: Rudnicki, R. (Ed.), Mathematical Modeling of Population Dynamics, Banach Center Publications, vol. 63. Warsa, Polish Academy of Science, pp. 47–86.

Dieckmann, U., Law, R., 1996. The dynamical theory of coevolution: a derivation from stochastic ecological processes. J. Math. Biol. 34, 579–612.

Doebeli, M., Dieckmann, U., 2000. Evolutionary branching and sympatric speciation caused by different types of ecological interactions. The Am. Nat. 156, S77–S101.

Doedel, E.J., Champneys, A.R., Fairgrieve, T.F., Kuznetsov, Y.A., Sandstede, B., Wang, X., 1997. Auto 97: Continuation and bifurcation software for ordinary differential equations. Technical Report, Concordia University, Montreal, Canada.

Droop, M.R., 1973. Some thoughts in nutrient limitation in algae. J. Phycol. 9, 264–272.

Geritz, S.A.H., Metz, J.A.J., Kisdi, E., Meszéna, G., 1997. Dynamics of adaptation and evolutionary branching. Phys. Rev. Lett. 78, 2024–2027.

Geritz, S.A.H., Kisdi, E., Meszéna, G., Metz, J.A.J., 1998. Evolutionarily singular strategies and the adaptive growth and branching of the evolutionary tree. Evol. Ecol. 12, 35–57.

Geritz, S.A.H., van der Meijden, E., Metz, J.A.J., 1999. Evolutionary dynamics of seed size and seedling competitive ability. Theoret. Popul. Biol. 55, 324–343.

Gragnani, A., Rinaldi, S., 1995. A universal bifurcation diagram for seasonally perturbed predator-prey models. Bull. Math. Biol. 57 (5), 701–712.

Hallam, T.G., Lassiter, R.R., Li, J., Suarez, L.A., 1990. Modelling individuals employing an integrated energy response: application to Daphnia. Ecology 71, 938–954.

Huisman, J., Weissing, F.J., 1999. Biodiversity of plankton by species oscillations and chaos. Nature 402, 407–410.

Huisman, J., Weissing, F.J., 2001. Biological conditions for oscillations and chaos generated by multispecies competition. Ecology 82 (10), 2682–2695.

Huisman, J., Weissing, F.J., 2002. Oscillations and chaos generated by competition for interactively essential resources. Ecol. Res. 17, 175–181.

Khibnik, A.I., Kuznetsov, Y.A., Levitin, V.V., Nikolaev, E.V., 1993. Continuation techniques and interactive software for bifurcation analysis of ODEs and iterated maps. Physica D 62, 360–371.

Kooi, B.W., Hanegraaf, P.P.F., 2001. Bi-trophic food chain dynamics with multiple component populations. Bull. Math. Biol. 63 (2), 271–299.

Kooi, B.W., Kooijman, S.A.L.M., 1999. Discrete event versus continuous approach to reproduction in structured population dynamics. Theoret. Popul. Biol. 56 (1), 91–105.

Kooi, B.W., Kooijman, S.A.L.M., 2000. Invading species can stabilize simple trophic systems. Ecol. Model. 133 (1–2), 57–72.

Kooi, B.W., Boer, M.P., Kooijman, S.A.L.M., 1999. Resistance of a food chain to invasion by a top predator. Math. Biosci. 157, 217–236.

Kooijman, S.A.L.M., 2000. Dynamic Energy and Mass Budgets in Biological Systems. Cambridge University Press, Cambridge.

Kot, M., Sayler, G.S., Schultz, T.W., 1992. Complex dynamics in a model microbial system. Bull. Math. Biol. 54, 619–648.

Matessi, C., Di Pasquale, C., 1996. Long term evolution of multi-locus traits. J. Math. Biol. 34, 613–653.

Metz, J.A.J., Geritz, S.A.H., Nisbet, R.M., 1992. How should we define 'fitness' for general ecological scenarios? Trends Ecol. Evol. 7, 198–202.

Metz, J.A.J., Geritz, S.A.H., Meszéna, G., Jacobs, F.J.A., van Heerwaarden, J.S., 1996. Adaptive dynamics, a geometrical study of the consequences of nearly faithful reproduction. In: Strien, S.J., van, Verduyn Lunel, S.M. (Eds.), Stochastic and Spatial Structures of Dynamical Systems. North-Holland, Amsterdam, pp. 183–231.

Mylius, S.D., Diekmann, O., 1995. On evolutionarily stable life histories, optimization and the need to be specific about density dependence. OIKOS 74 (2), 218–224.

Noonburg, E.G., Nisbet, R.M., Mccauley, E., Gurney, W.S.C., Murdoch, W.W., deRoos, A.M., 1998. Experimental testing of dynamic energy budget models. Funct. Ecol. 12 (2), 211–222.

Shertzer, K.W., Ellner, S.P., 2002. Energy storage and the evolution of population dynamics. J. Theoret. Biol. 215, 183–200.

Smith, H.L., Waltman, P., 1994. The Theory of the Chemostat. Cambridge University Press, Cambridge.

Tilman, D., 1982. Resource Competition and Community Structure. Princeton University Press, Princeton.